Identification of simplified energy performance models of variable-speed air conditioners using likelihood ratio test method

MAOMAO HU[1,2], FU XIAO[1,*], HOWARD CHEUNG[3]

[1]*Department of Building Services Engineering, The Hong Kong Polytechnic University, Kowloon, Hong Kong*

[2] *Research Institute for Sustainable Urban Development, The Hong Kong Polytechnic University, Kowloon, Hong Kong*

[3] *Carbon Exchange (Hong Kong) Limited, Hong Kong Science Park, Hong Kong*

Abstract

Variable-speed air conditions (ACs) are gradually replacing single-speed ACs in residential buildings in densely populated cities like Hong Kong due to better control accuracy and higher energy efficiency at part-load conditions. Simplified energy performance models of variable-speed ACs are needed for different purposes, including building energy analysis, model-based fault detection and diagnosis, and model-based optimal control. However, how to identify the most suitable model from a series of candidate models with various complexities is rarely discussed. This study presents a model selection approach based on the likelihood ratio test (LRT) method to identify the most suitable energy performance model of variable-speed ACs. A full model and a range of reduced models/sub-models for variable-speed ACs are first formulated for model selection procedure. Maximum likelihood estimation method is applied to estimate the parameters in each candidate model. Performances of the candidate models in each step of the selection process are compared using LRTs. Test results demonstrate that the model selection approach can effectively select the cooling capacity and COP models for a typical variable-speed AC with reasonable complexity and satisfactory accuracy. The root mean square errors of the selected models of cooling capacity factor and COP factor are 0.0188 and 0.0463, respectively.

Keywords: Variable-speed air conditioners; Maximum likelihood estimation; Likelihood ratio test; Model selection; Building energy analysis.

***Maomao Hu**, **PhD**, is a Post-Doctoral Fellow. **Fu Xiao**, **PhD**, Member ASHRAE, is an associate Professor. **Howard Cheung, PhD,** is a Technical & Research Manager.*

**Corresponding author e-mail: linda.xiao@polyu.edu.hk*

Introduction

Ductless split air conditioners (ACs) are widely installed in high-rise residential buildings in high-density urban cities, especially, the cities in Asia like Hong Kong and Shanghai. They account for around 36% of the total electricity consumption in the residential sector in Hong Kong in 2015 (EMSD, 2018). Energy management and control of residential ACs have great potential to provide energy savings (Siddiqui, 2009) and demand response resources (FERC, 2009, 2018). Energy performance models of ACs are usually needed for building energy performance assessment (Thomas et al., 2012; W. Wang et al., 2019; Hu & Xiao, 2018) as well as model-based fault detection and diagnosis (FDD) (Y. Li et al., 2015; Guo et al., 2017) and model-based optimal control (Hu & Xiao, 2018; Hu et al., 2019). In recent years, due to the improved energy efficiency at part-load conditions, the single-speed type ACs have gradually been replaced by variable-speed type ACs in residential and small and medium-sized commercial buildings in Asia. In Japan, the variable refrigerant flow systems account for around 50% of the medium-sized commercial buildings (Aynur, 2010). The variable-speed ACs can operate under variable frequencies and provide a wide range of cooling capacities to meet the changing cooling demands more quickly and efficiently. With the wider applications of variable-speed ACs, simplified energy performance models of this type of ACs, which are computationally efficient yet accurate, are required for building energy modeling, model-based FDD and model-based optimal control.

Energy performance models of ACs can be classified into physical models and simplified empirical models. For both physical and empirical models, they can be further classified into transient and steady-state models. Steady-state AC models are competent to simulate the coupled dynamic behaviors of an air conditioned room under time-varying internal and external operating conditions since refrigerant dynamics in ACs are much quicker than the building thermal dynamics (B. P. Rasmussen, 2005). Many studies adopted steady-steady AC models for energy performance analysis of either individual room/building or building clusters. Yoon et al. (2014) adopted the AC power consumption model in EnergyPlus to investigate the effects of temperature set-point reset strategies on the power reductions of residential AC systems. The power consumption model was a linear function of the temperature difference between the indoor air temperature and temperature set-point. S. Li et al. (2014) investigated and compared different demand response (DR) strategies under the disturbances of dynamic pricing

tariffs, seasons and weather using building simulation software eQUEST in which the cooling capacity and energy efficiency ratio of AC were both fixed. Besides the energy performance evaluation of an individual dwelling, the single-speed AC model was also used to estimate the DR potential at a cluster/neighborhood level, which is essential for electric utilities to make decisions on grid operations, such as the dynamic electricity pricing (Faruqui & Sergici, 2010) and spinning reserve (D. Wang et al., 2013). Taniguchi et al. (2016) employed the bottom-up method to evaluate the effects of electricity saving measures on peak demand reductions in the Japanese residential sector with 5000 households. The coefficient of performance (COP) of residential ACs was estimated based on the outdoor air temperature and the rated COP. An AC power consumption model was developed to evaluate the impacts of various residential AC control strategies on the electric distribution feeders during DR periods (Lu, 2012; Zhang et al., 2013). The AC power consumption was converted from the thermal load by using the part-load performance data provided by manufacturers. The part-load performance data for AC units of different sizes were assumed to be identical.

Model-based FDD and model-based optimal control of split ACs were also widely researched. Thomas et al. (2012) developed an intelligent model-based AC controller which can realize optimal comfort and cost trade-offs during on-peak hours. The cooling capacity and COP of the AC were represented as the functions of outdoor air temperature and performance data under rated operating conditions. Chen et al. (2012) managed the residential appliances based on real-time electricity prices using stochastic optimization and robust optimization. A simple formula was used to describe the relationship among the outdoor air temperature, indoor air temperature and AC power consumption. Alibabaei et al. (2016) developed a MATLAB-TRNSYS co-simulator to apply different predictive strategy planning models on residential HVAC system. The COP model for the air-source heat pump solely depended on the outdoor air temperature.

In the above-mentioned residential AC models adopted in a diversity of applications, the models are only applicable to single-speed ACs. A major difference between single-speed ACs and variable-speed ACs is that the performances of variable-speed ACs are influenced not only by the indoor and outdoor operating conditions, but also by the operating frequencies of compressors. Table 1 lists the empirical performance models of variable-speed ACs developed in previous studies. Y. Li et al. (2015) proposed a

compressor power model for a variable-speed rooftop unit (RTU) based on theoretical and experimental analyses for performance evaluation and real-time FDD. The compressor model had a relative error of ±8% under normal operation conditions . Shao et al. (2004) developed the energy performance models for variable-speed compressors at two steps, i.e., development of the model at the basic frequency and correction of the model by the compressor frequency. The performance data from compressor manufacturers were used to identify the model, which produced a 3% relative error for compressor power input. Cai and Braun (2018) developed performance models of a variable-speed RTU based on the ASHRAE Toolkit model (Brandemuehl, 1993) to predict the unit's performance under various weather conditions, compressor speeds and supply fan speeds. The models were then used to investigate the energy and cost saving potential for the retrofit of RTU with variable-speed driver. Cheung and Braun (2010) proposed an empirical modeling approach for variable-speed ductless heat pumps, which consisted two parts: 1) modeling the performance at maximum compressor speed; and 2) modeling the performance with the relative load. The polynomial regression models were identified based on steady-state performance data and simplified by statistical methods. Guo et al. (2017) proposed a power model of variable-speed compressor with 20 coefficients, which was used as a virtual power sensor for FDD of variable refrigerant flow system.

Table 1. Summary of empirical performance models (power or cooling capacity) of variable-speed ACs

`	Model mathematical representation	No. of variables	No. of parameters
Shao et al. (2004)	$W = (\beta_0 + \beta_1 T_{evap} + \beta_2 T_{cond} + \beta_3 T_{evap}^2 + \beta_4 T_{cond}^2 + \beta_5 T_{evap} T_{cond})$ $(\beta_6 + \beta_7 (N_{comp} - N_{comp,rated}) + \beta_8 (N_{comp} - N_{comp,rated})^2)$	3	9
Cheung and Braun (2010)	$\frac{W}{W_{max}} = \beta_0 + \beta_1 \frac{Q}{Q_{max}} + \beta_2 \left(\frac{Q}{Q_{max}}\right)^2 + \beta_3 \frac{Q}{Q_{max}} \frac{V}{V_{max}} + \beta_4 \left(\frac{Q}{Q_{max}}\right)^3$ $+\beta_5 \left(\frac{V}{V_{max}}\right)^3 + \beta_6 \frac{Q}{Q_{max}} \left(\frac{V}{V_{max}}\right)^2$ $where\ W_{max} = \alpha_0 + \alpha_1 T_{out,db};\ Q_{max} = \alpha_2 + \alpha_3 T_{out,db}$	3	11
Y. Li et al. (2015)	$W = \beta_0 + \beta_1 T_{out,db} + \beta_2 N_{comp} + \beta_3 T_{out,db} N_{comp}$	2	4
Guo et al. (2017)	$W = \beta_0 + \beta_1 T_{evap} + \beta_2 T_{cond} + \beta_3 N_{comp} + \beta_4 T_{evap}^2 + \beta_5 T_{cond}^2$ $+\beta_6 N_{comp}^2 + \beta_7 T_{evap} T_{cond} + \beta_8 T_{evap} N_{comp} + \beta_9 T_{cond} N_{comp} + \beta_{10} T_{cond}^3$ $+\beta_{11} T_{evap}^3 + \beta_{12} N_{comp}^3 + \beta_{13} T_{evap}^2 T_{cond} + \beta_{14} T_{evap}^2 N_{comp} + \beta_{15} T_{cond}^2 T_{evap}$ $+\beta_{16} T_{cond}^2 N_{comp} + \beta_{17} N_{comp}^2 T_{evap} + \beta_{18} N_{comp}^2 T_{cond} + \beta_{19} T_{cond} T_{evap} N_{comp}$	3	20
Cai and Braun (2018)	$\frac{Q_{cap}}{Q_{cap,rated}} = (\beta_0 + \beta_1 T_{in,wb} + \beta_2 T_{in,wb}^2 + \beta_3 T_{out,db} + \beta_4 T_{out,db}^2 + \beta_5 T_{in,wb} T_{out,db})$ $(1 + \beta_6 \frac{V}{V_{rated}} + \beta_7 \left(\frac{V}{V_{rated}}\right)^2)(1 + \beta_8 N_{comp} + \beta_9 N_{comp}^2 + \beta_{10} N_{comp}^3)$	4	11

Most existing energy performance models of variable-speed ACs are more or less the same as those listed in Table 1, which have different levels of complexities with the number of the undetermined

parameters ranging from 4 -20. The question that to what extent the complexity of the energy performance models should be to achieve satisfactory accuracy has not yet been addressed. Balancing the model complexity and model accuracy is a critical issue for model development. To avoid under-fitting or over-fitting, the model needs to have a suitable complexity in agreement with the level of information embedded in data (Bacher & Madsen, 2011). Yu et al. (2018) used the Bayesian Information Criteria to develop the stepwise regression model for mist precooling process for an air-cooled chiller. The unknown parameters in the models were penalized to avoid the overfitting problem. Backward elimination and Mallows's C_p statistic method was used in Cheung's work (Cheung & Braun, 2010) to simplify to the performance model of a heat pump system operating in heating mode. A reliable model selection approach is needed to identify the most suitable model for residential variable-speed ACs.

This study aims to develop a model selection approach to identify the most suitable energy performance model for variable-speed ACs, which can be used in building energy modeling as well as model-based FDD and optimal control strategies in smart home energy management systems. The main contributions of this study include: 1) A full model and a series of candidate reduced models/sub-models for variable-speed ACs are formulated to characterize their performances under various operating frequencies and operating conditions; 2) A model selection approach is designed to identify the most suitable model. In each step of the selection process, the candidate models are compared using likelihood ratio tests. Maximum likelihood estimation method is applied to estimate the parameters of each candidate model. 3) A typical split-type variable-speed AC is chosen to conduct the case study and to test the model selection approach. The candidate models of cooling capacity and COP are evaluated and compared using various performance metrics.

The remainder of this paper is organized as follows. The methodology section first introduces the statistical methods adopted for model selection, including the likelihood ratio test and maximum likelihood estimation. Based on these two methods, a generic model selection approach is then designed. After that, the full model and candidate sub-models of variable-speed ACs are presented in this section for model selection. In the section of test and evaluation, a typical variable-speed AC is chosen to test the model selection approach developed for identifying the most suitable energy performance models for cooling capacity and COP of the variable-speed AC. The performances of the models are evaluated using

various metrics. Finally, major research findings and conclusions are presented in the section of conclusions.

Methodology

Likelihood ratio test method for model selection

Model selection is the process of selecting the most suitable model from a set of candidate models using statistical inference techniques, given a series of observations. Likelihood ratio test (LRT) is one of the most popular statistical model selection methods (Casella & Berger, 2002). The main idea of LRT is to compare the goodness of fit of two statistical models, i.e., a null model (representing the null hypothesis H_o) against an alternative model (representing an alternative hypothesis H_1), by using the ratio λ of the likelihoods of the two models (Pawitan, 2001). The implementation of LRT is based on likelihood function and maximum likelihood estimation (MLE), which are also prerequisites for chi-square test, Bayesian methods and some model selection criteria like the Akaike information criterion (Myung, 2003). Bacher and Madsen (2011) used LRT to identify the most suitable model to characterize the thermal dynamic of the building. A forward selection procedure was developed to select the suitable model among a series of models of increasing complexities. Before the application to AC model selection, the fundamentals behind the MLE and LRT are first briefly introduced in this section.

Maximum likelihood estimation of parameters

Maximum likelihood estimation is used to estimate the undetermined parameters in the statistical models. Given a statistical model Eq. (1) and the observations $\{(X_1, Y_1), \quad (X_2, Y_2), \quad \cdots \quad (X_n, Y_n)\}$, the likelihood function, i.e., the joint probability density, then can be represented as shown in Eq. (2).

$$Y = f(X, \alpha) + \varepsilon_Y \tag{1}$$

$$L(\alpha, \sigma_Y^2 | Y_i) = \prod_{i=1}^{n} p(Y_i | X_i; \alpha, \sigma_Y^2) = \prod_{i=1}^{n} \frac{1}{\sqrt{2\pi\sigma_Y^2}} e^{-\frac{(Y_i - f(X_i, \alpha))^2}{2\sigma_Y^2}} \tag{2}$$

Where X, α and Y are the vectors of variable, parameter and measurement, respectively; ε_Y denotes the measurement errors, which are assumed to be Gaussian white noise processes with variances σ_Y^2, i.e., $\varepsilon_Y \sim N(0, \sigma_Y^2)$; $p(Y_i | X_i; \alpha, \sigma_Y^2)$ is the conditional probability density function of Y for each X given the

parameters α and σ_Y^2. For computational convenience, the likelihood function Eq. (2) can be transformed to log-likelihood function Eq. (3).

$$lnL(\alpha, \sigma_Y^2|Y_i) = -\frac{n}{2}ln2\pi - nln\sigma_Y - \frac{1}{2\sigma_Y^2}\sum_{i=1}^{n}(Y_i - f(X_i, \alpha))^2 \quad (3)$$

The maximum likelihood estimates of the parameters are then found by Eq. (4). A nonlinear optimization algorithm can be applied to maximize it and calculate the maximum likelihood estimates.

$$\hat{\alpha} = \underset{\alpha}{\text{argmax}}\{lnL(\alpha, \sigma_Y^2|Y_i)\} \quad (4)$$

Likelihood ratio test

Likelihood ratio test is a type of hypothesis test. It is specifically used to choose the "best" model between two nested models, while the ordinary hypothesis tests (e.g., Z-test, T-test and Chi-square test) are normally used to test whether an independent variable has certain effects on the dependent variable. For better description of the LRT method, some terms used in this study are first defined here, including full model, reduced model/sub-model and larger model. In the field of model regression, a full model denotes the statistical model which includes all the possible influential terms, while a reduced model/sub-model only includes some terms of the full model. When a model has a larger number of parameters, we call it the larger model. The models with reduced/fewer terms in the larger model are called the reduced model/sub-model of the larger model.

Let a larger model have parameters $\alpha \in \Omega$, where the number of the parameters in the larger model $\mathrm{m} = \dim(\Omega)$. The sub-model of the larger model has parameter $\alpha \in \Omega_0$, where the number of the parameters in the sub-model $\mathrm{r} = \dim(\Omega_0)$ and $\Omega_0 \in \Omega$, i.e., $r < m$. Then, the statistical hypothesis testing can be described by Eq. (5), which can be tested by the LRT, as shown in Eq. (6).

$$H_0: \alpha \in \Omega_0 \quad \text{vs.} \quad H_1: \alpha \in \Omega \backslash \Omega_0 \quad (5)$$

$$\lambda(X_i) = \frac{sup\{L(\alpha|X_i): \alpha \in \Omega_0\}}{sup\{L(\alpha|X_i): \alpha \in \Omega\}} \quad (6)$$

where *sup* denotes the supremum function. The likelihood ratio λ expresses how more likely the observations are under the sub-model than the larger model. Under the null hypothesis H_0, the test statistic $-2\ln(\lambda(X_i))$ is asymptotically χ^2 distributed with $(\mathrm{m} - \mathrm{r})$ degrees of freedom. If H_0 is rejected, it means the likelihood of the larger model is significantly larger than the likelihood of the candidate sub-model, and the sub-model cannot be used to replace the larger model to better describe the

information embedded in observed data. Test statistical *p*-value under χ^2 distribution is commonly used as a critical value to determine whether to reject the candidate sub-model in favor of the larger model. Thus, the LRT is sometimes called the likelihood-ratio chi-squared test. The significance level of the test is commonly set as 0.05.

Model selection procedure and model evaluation

Fig. 1 shows the flowchart of the whole model selection approach. In the first iteration of the statistical hypothesis testing, the full model M_{full} is used as the larger model under the alternative hypothesis H_1, while its restricted sub-models are used as the models under the null hypothesis H_0. If no sub-models exist, then the model selection process ends. If the sub-models exist, the larger model is tested down against its multiple sub-models using LRTs after the parameters being estimated using MLE. The comparison process in each iteration stops when the test result starts to have a p-value smaller than 0.05. If there is no sub-model with a p-value larger than 0.05, the larger model under the alternative hypothesis H_1 is chosen as the most suitable model, otherwise the restricted sub-model with the largest p-value is selected as the most suitable model in that iteration. The most suitable model in previous iteration is used as the larger model under H_1 in next iteration to compare with its restricted sub-models. The whole selection process stops when no sub-models of the larger model can be found.

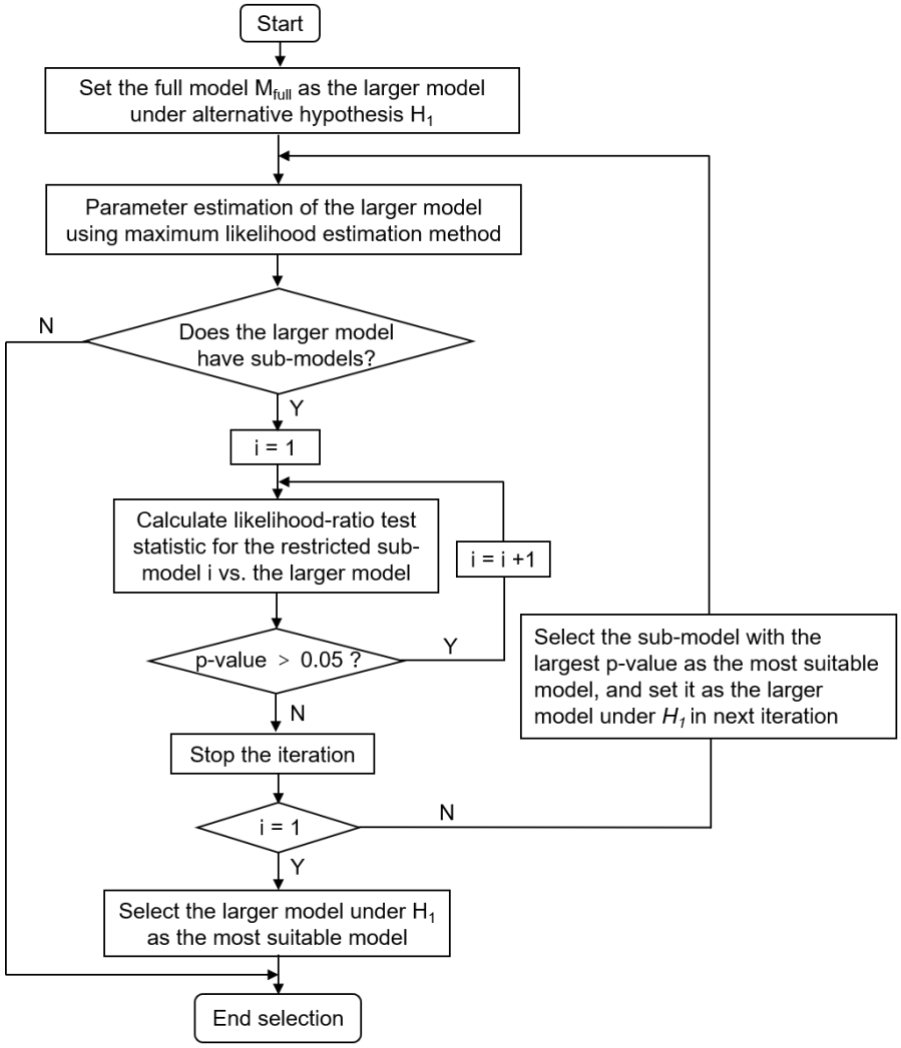

Fig. 1. Flowchart of the model selection approach

The models selected in each iteration are evaluated by various performance metrics, including the root mean square errors (RMSE), the coefficient of determination (R^2) and the coefficient of variance (CV), as shown in Eqs. (7) – (9), respectively. The RMSE is an effective measure to characterize how accurately the model predicts the response, which indicates the absolute fitness of the model to the observed dataset. The R^2 is intuitively scaled to between 0 and 1, which indicates the goodness of the fit regression. The CV is a dimensionless number and is also known as relative standard deviation, which is defined as the ratio of the standard deviation to the mean.

Root mean square errors

$$\mathrm{RMSE} = \sqrt{\frac{1}{n}\sum_{i=1}^{n}(Y_{sample,i} - Y_{model,i})^2} \tag{7}$$

Coefficient of determination

$$R^2 = 1 - \frac{\sum_{i=1}^{n}(Y_{sample,i} - Y_{model,i})^2}{\sum_{i=1}^{n}(Y_{sample,i} - \bar{Y})^2} \tag{8}$$

Coefficient of variation

$$CV = \frac{\sqrt{\frac{1}{n}\sum_{i=1}^{n}(Y_{sample,i}-Y_{model,i})^2}}{\bar{Y}} \quad (9)$$

Model specifications for variable-speed ACs

Full model

The energy performance a single-speed AC can be characterized by dimensionless factors (Q^* and COP^*) of cooling capacity (Q) and coefficient of performance (COP), which are the ratios of the performance data on a given environmental condition to the rated Q and COP (Q_{rated} and COP_{rated}) Environmental conditions normally include dry-bulb and wet-bulb temperatures of both indoor air ($T_{in,db}$ and $T_{in,wb}$) and outdoor air ($T_{out,db}$ and $T_{out,wb}$). Experimental studies show that the thermal and energy performances of single-speed AC are mainly influenced by the outdoor air dry-bulb temperature ($T_{out,db}$) and indoor air wet-bulb temperature ($T_{in,wb}$) (Cherem-Pereira & Mendes, 2012; Meissner et al., 2014). Thus, as shown in Eqs. (10) - (11), Q^* and COP^* of single-speed ACs are normally represented as the polynomial functions of indoor air wet-bulb temperature ($T_{in,wb}$) and outdoor air dry-bulb temperature ($T_{out,db}$).

$$Q^* = \frac{Q}{Q_{rated}} = a_1 + a_2T_{in,wb} + a_3T_{out,db} + a_4T_{in,wb}^2 + a_5T_{out,db}^2 + a_6T_{in,wb}T_{out,db} + \varepsilon_Q \quad (10)$$

$$COP^* = \frac{COP}{COP_{rated}} = b_1 + b_2T_{in,wb} + b_3T_{out,db} + b_4T_{in,wb}^2 + b_5T_{out,db}^2 + b_6T_{in,wb}T_{out,db} + \varepsilon_{COP} \quad (11)$$

where ε_Q and ε_{COP} are the measurement errors for cooling capacity factor and COP factor, which are assumed to be Gaussian white noise processes with variances σ_Q^2 and σ_{COP}^2, respectively. Note that Eqs. (10) – (11) are linear, although they have the quadratic items. That is because in statistics, a regression model is called linear if all terms in the model are represented as a parameter multiplied by an independent variable.

As listed in Table 1, the common feature among the existing performance models of variable-speed ACs was that they all captured the effects of not only the environmental conditions but also the operating speed of compressor on energy performances. Compared with the models in (Shao et al., 2004; Cai & Braun, 2018), Guo's model (Guo et al., 2017) had much more coefficients, because it was represented in the form of expansion, i.e., the terms in each bracket was multiplied out, which added the model complexity. In the light of the structure of single-speed AC models and the existing variable-speed

models in Table 1, the full version of the energy performance models for variable-speed ACs are proposed for model selection in this study as shown in Eqs. (12) – (13). Different from the linear energy performance models of single-speed ACs, the energy performance models of variable-speed ACs are nonlinear due to the cross-coupling interactions existing among different coefficients. The nominal performance of variable-speed AC is rated not only by the environmental variables but also by the operating frequency, e.g., N_{comp} = 50 Hz, $T_{in,wb}$ = 19.4 ℃ and $T_{out,db}$ = 35 ℃.

$$Q^* = \frac{Q}{Q_{rated}} = \left(a_1 + a_2 T_{in,wb} + a_3 T_{out,db} + a_4 T_{in,wb}^2 + a_5 T_{out,db}^2 + a_6 T_{in,wb} T_{out,db}\right) \times \left(1 + b_1 N_{comp} + b_2 N_{comp}^2 + b_3 N_{comp}^3\right) + \varepsilon_Q \quad (12)$$

$$COP^* = \frac{COP}{COP_{rated}} = \left(c_1 + c_2 T_{in,wb} + c_3 T_{out,db} + c_4 T_{in,wb}^2 + c_5 T_{out,db}^2 + c_6 T_{in,wb} T_{out,db}\right) \times \left(1 + d_1 N_{comp} + d_2 N_{comp}^2 + d_3 N_{comp}^3\right) + \varepsilon_{COP} \quad (13)$$

The energy performance models of variable-speed ACs are black-box models, in which the coefficients need to be identified using performance data under various environmental conditions ($T_{in,wb}$ and $T_{out,db}$) and operating frequencies (N_{comp}). Since the cooling capacity model and COP model have the same structure, only the cooling capacity model is used as an example for parameter estimation here. The statistical cooling capacity model is given by Eq. (14). Given the observations $\{(X_1, Q_1^*), \ (X_2, Q_2^*), \ \cdots \ (X_n, Q_n^*)\}$, the log-likelihood function and the maximum likelihood estimates of the parameters are given by Eq. (15) and Eq. (16), respectively.

$$Q^* = f(X, \alpha) + \varepsilon_Q \quad (14)$$

$$lnL\left(\alpha, \sigma_Q^2 \middle| Q_i^*\right) = -\frac{n}{2} ln2\pi - nln\sigma_Q - \frac{1}{2\sigma_Q^2} \sum_{i=1}^{n} (Q_i^* - f(X_i, \alpha))^2 \quad (15)$$

$$\hat{\alpha} = \underset{\alpha}{\operatorname{argmax}} \{lnL\left(\alpha, \sigma_Q^2 \middle| Q_i^*\right)\} \quad (16)$$

where $\mathrm{X} = [T_{in,wb} \quad T_{out,db} \quad N_{comp}]$; $\alpha = [a_1 \quad a_2 \quad \cdots \quad a_6; \quad b_1 \quad b_2 \quad b_3]$ and $\varepsilon_Q \sim N(0, \sigma_Q^2)$.

Candidate sub-models

Before the model selection process using statistical hypothesis testing method, the complex model is first transformed into smaller sub-models by imposing constraints on the parameters. As shown in Table 2, Eq. (12) is used as the full and unrestricted model (M_1) for cooling capacity factor Q^* in this study. It consists of 9 undetermined parameters in total, including 3 parameters (i.e., b_1 - b_3) in the terms of compressor speed (N_{comp}) and 6 parameters (i.e., a_1 - a_6) in the terms of air temperatures ($T_{in,wb}$ and $T_{out,db}$), respectively. Different levels of constrains are then imposed on the terms to form the candidate

sub-models (M_2 – M_{12}) with a hierarchy of complexities. Specifically, the number of the N_{comp} term is decreased from 3 (cubic function, $\forall b_j \neq 0, j \in [1,2,3]$) to 2 (quadratic function, $b_3 = 0$) and 1 (linear function, $b_2 = b_3 = 0$). For each type of N_{comp} term, the number of the temperature term is decreased from 6 ($\forall a_i \neq 0, i \in [1, 2, \dots, 6]$) to 5 ($a_6 = 0$), 4 ($a_5 = a_6 = 0$) and 3 ($a_4 = a_5 = a_6 = 0$), respectively.

Table 2. Specifications of full model and sub-models for the cooling capacity factor Q^* of variable-speed ACs

Model type	Model number	Parameters in the term of N_{comp}	Parameters in the term of $T_{in,wb}$ and $T_{out,db}$	No. of parameters
Full model	M_1	$\forall b_j \neq 0, j \in [1,2,3]$	$\forall a_i \neq 0, i \in [1, 2, \dots, 6]$	9
Candidate sub-models	M_2		$a_6 = 0$	8
	M_3		$a_5 = a_6 = 0$	7
	M_4		$a_4 = a_5 = a_6 = 0$	6
	M_5	$b_3 = 0$	$\forall a_i \neq 0, i \in [1, 2, \dots, 6]$	8
	M_6		$a_6 = 0$	7
	M_7		$a_5 = a_6 = 0$	6
	M_8		$a_4 = a_5 = a_6 = 0$	5
	M_9	$b_2 = b_3 = 0$	$\forall a_i \neq 0, i \in [1, 2, \dots, 6]$	7
	M_{10}		$a_6 = 0$	6
	M_{11}		$a_5 = a_6 = 0$	5
	M_{12}		$a_4 = a_5 = a_6 = 0$	4

Test and evaluation

Description of the AC and performance data generated from physical models

A number of experimental studies of steady-state performances of ACs have been carried out (Cherem-Pereira & Mendes, 2012; Meissner et al., 2014; Gayeski, 2010). Gayeski (2010) produced quite elaborate experiment data for a Mitsubishi split-type variable-speed air conditioner with a rated cooling capacity of 2.5kW. It is one of the most popular types of residential variable-speed ACs and the main specifications are listed in Table 3. The same split-type variable-speed air conditioner was chosen for performance identifications under a wide range of typical operating conditions. AC manufacturers seldom provide enough performance data in the full range of operating conditions. Therefore, the physical models are developed in this study to obtain complete performance data of the typical ductless split variable-speed AC. The detailed physical models of each components of variable-speed ACs as well as the numerical solution are provided in Appendix.

Table 3. Main specifications of the variable-speed AC

Item		Specification
Refrigeration		R410A
Compressor	type	rotary piston type
	piston displacement volume (cm^3)	10
EEV	type	step motor
	inner diameter (mm)	4
Evaporator	dimension (L×W×H) (m)	0.62×0.03×0.34
	row number	2
	loop number	2
	tube number per row	16
	tube length per row (m)	0.62
	tube outer diameter (mm)	6.8
	tube inner diameter (mm)	5.2
	fin number	488
	fin pitch (mm)	1.17
	fin thickness (mm)	0.102
Condenser	dimension (L×W×H) (m)	0.86×0.5×0.022
	row number	1
	loop number	2
	tube number per row	12
	tube length per row (m)	0.86
	tube outer diameter (mm)	6.5
	tube inner diameter (mm)	4.9
	fin number	610
	fin pitch (mm)	1.34
	fin thickness (mm)	0.0762

With the steady-state physical model of the variable-speed AC, the dimensionless factors of cooling capacity and COP (Q^* and COP^*) of the target variable-speed AC under typical operating conditions are obtained. The typical operating conditions are the combinations of typical compressor rotational speeds ($N_{comp,ty}$ = [20, 30, … , 100]), typical dry-bulb temperature of outdoor air ($T_{out,db,ty}$ = [23, 26, 29, 32, 35, 38]) and typical wet-bulb temperature of indoor air ($T_{in,wb,ty}$ = [14.6, 17.1, 19.4, 22.0, 24.5, 27.0]). The corresponding typical dry-bulb temperature of the indoor air $T_{in,db,ty}$ is [21, 24, 27, 30, 33, 36]. As shown in Fig. 2, the cooling capacity and COP of variable-speed AC mainly depend on the compressor speed. With the increase of compressor speed, the cooling capacity increases, but the COP decreases. The cooling capacity increases with the increase of indoor air temperature and decreases with the increase of the outdoor air temperature.

To validate the performance data generated by the physical modeling method, 40 sets of experimental data by Gayeski (2010) are compared with the modeled data under the same operating conditions. Fig. 3 shows the comparisons between the modeled data and the experimental data. The deviations are mainly in the range of ±15%. The mean absolute percentage errors (MAPEs) between the predicted and tested

cooling capacity and COP are 5.56% and 11.94%, respectively. In the next section, the steady-state performance data of the typical variable-speed AC are used for the model identification.

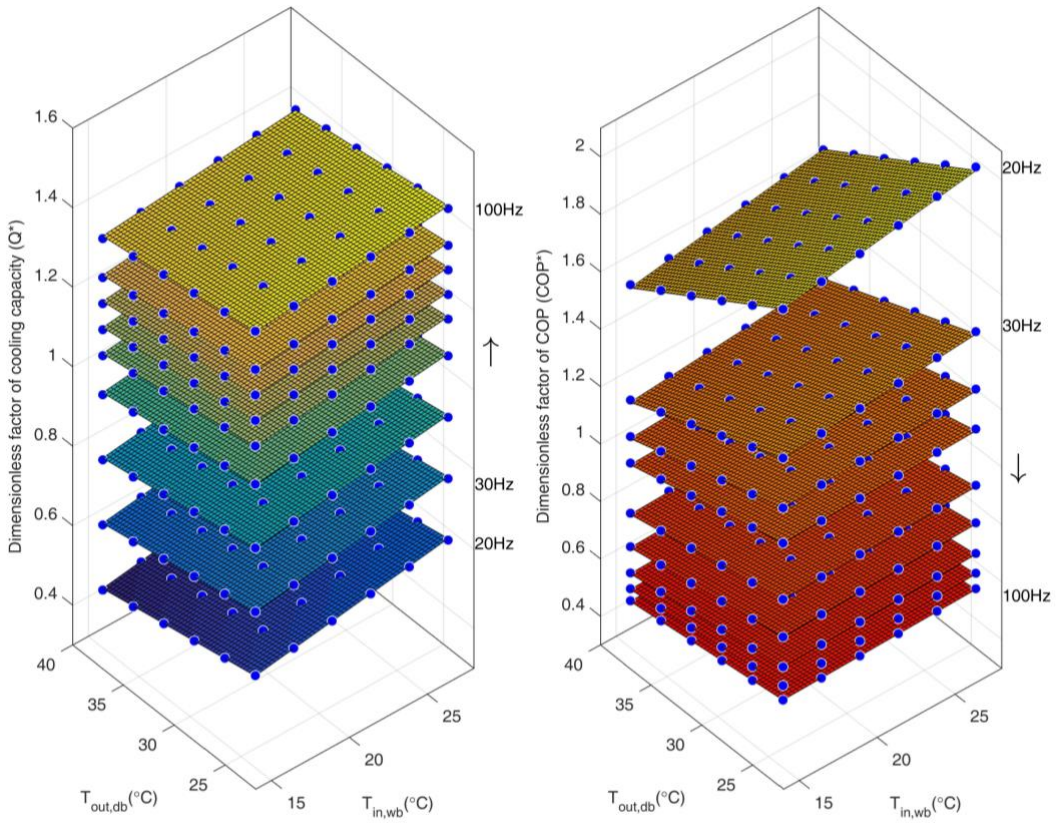

Fig. 2. Performance data (dimensionless factors of cooling capacity and COP) of the variable-speed AC under typical operating conditions.

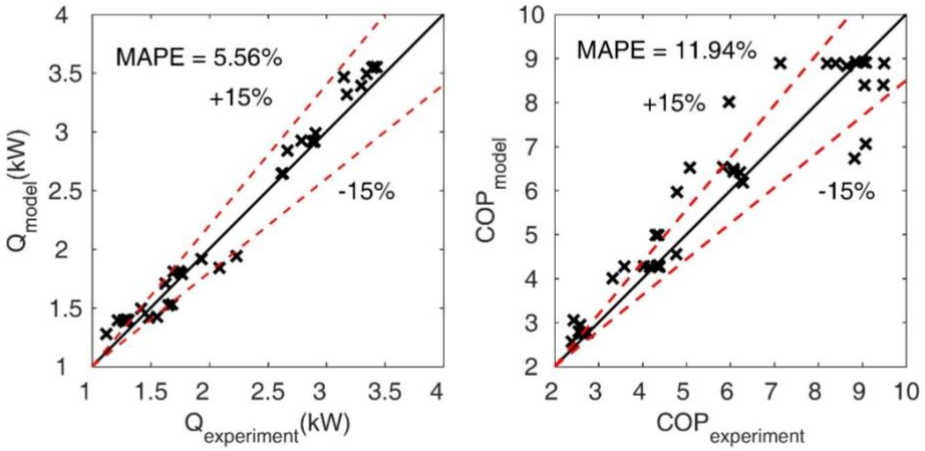

Fig. 3. Comparisons between the modeled data and experimental data of the typical variable-speed AC.

Model identification and model evaluation

With the performance data under various operating conditions, the model selection procedure can be applied to find the most suitable model for variable-speed ACs. The whole energy performance models of variable-speed ACs consist of the cooling capacity model (Q^*) and the COP model (COP^*), which are identified and evaluated in the following subsections, respectively.

Identification and evaluation of the cooling capacity model

Table 4 lists the log-likelihoods of tested cooling capacity models in each iteration step. As illustrated in Fig. 1, the selection procedure begins with the full and unrestricted model M_1, i.e., Eq. (12). In the first iteration, the full model M_1 acts as the larger model under the alternative hypothesis H_1, and is compared with its restricted sub-models, i.e., M_2 – M_{12}. The first iteration stops at the test of M_5 since it starts to have a p-value below 0.05, which indicates a strong evidence to reject the sub-model under the null hypothesis. After the first iteration, M_4 is selected as the most suitable model among the alternative sub-models since it has the largest p-value, i.e., 0.0974, and the minimum number of parameters, i.e., 6.

In the second iteration, M_4 is regarded as the larger model under the alternative hypothesis H_1, and is compared with its restricted sub-models, i.e., M_8 and M_{12}. Since the p-value is below 0.05 for the test of M_8 vs. M_4, the iteration stops, and M_8 with the likelihood value of 752.81 is rejected to replace M_4. Thus, the whole selection process for cooling capacity model ends up with M_4 as the sufficient model. Specifically, the identified most suitable cooling capacity model for variable-speed ACs is given by Eq. (17).

$$Q^* = \frac{Q}{Q_{rated}} = \left(a_1 + a_2 T_{in,wb} + a_3 T_{out,db}\right) \times \left(1 + b_1 N_{comp} + b_2 N_{comp}^2 + b_3 N_{comp}^3\right) + \varepsilon_Q \qquad (17)$$

The parameter estimates and performance indicators for all candidate Q^* model is also listed in Table 5. As can be seen from the table, the parameter estimates are different in various candidate Q^* models. Compared with M_5 and M_8, M_1- M_4 of Q^* have almost the same accuracy (RMSE and CV) and fitness (R^2) to the data. The RMSE, CV and R^2 for M_4 of Q^* are 0.0463, 0.0479 and 0.9867, respectively. However, M_4 has the smallest number of parameters, i.e., 6. The results show that the proposed model selection approach can efficiently help to select the feasible model to characterize the cooling capacity performance of variable-speed ACs.

Table 4. Likelihood ratio test results in the selection of cooling capacity (Q^*) model.

Iteration	Properties	Larger unrestricted model under H_1	Restricted sub-models under H_0			
0	Model number	M_1				
	No. of parameters	9				
	Log-likelihood	835.64				
1	Model number	M_1	M_2	M_3	M_4	M_5
	No. of parameters	9	8	7	6	8
	Degrees of freedom	/	1	2	3	1
	Log-likelihood	835.64	834.09	833.07	832.49	755.35
	p-value	/	0.0786	0.0764	0.0974	$<10^{-16}$
2	Model number	M_4	M_8			
	No. of parameters	6	5			
	Degrees of freedom	/	1			
	Log-likelihood	832.49	752.81			
	p-value	/	$<10^{-16}$			

Table 5. Parameter estimates and performance indicators for the candidate cooling capacity (Q^*) models.

		Model					
		M_1	M_2	M_3	M_4	M_5	M_8
Parameter estimates	a_1	0.0073	0.0070	0.0190	0.0050	0.1791	0.1812
	a_2	2.92×10^{-5}	4.29×10^{-5}	0.0001	2.01×10^{-5}	0.0007	0.0007
	a_3	-2.24×10^{-5}	-1.29×10^{-5}	-7.62×10^{-5}	-1.98×10^{-5}	-0.0006	-0.0007
	a_4	-3.25×10^{-7}	-3.24×10^{-7}	-8.52×10^{-7}	/	-8.03×10^{-6}	/
	a_5	-2.62×10^{-7}	-2.61×10^{-7}	/	/	-6.47×10^{-6}	/
	a_6	4.52×10^{-7}	/	/	/	1.11×10^{-5}	/
	b_1	4.5062	4.5197	1.6737	6.6236	0.1188	0.1188
	b_2	-0.0418	-0.0419	-0.0152	-0.0616	-0.0005	-0.0005
	b_3	0.0002	0.0002	5.88×10^{-5}	0.0002	/	/
Performance indicators	*RMSE*	0.0188	0.0188	0.0189	0.0188	0.0241	0.0241
	R^2	0.9950	0.9954	0.9953	0.9954	0.9924	0.9924
	CV	0.0180	0.0179	0.0180	0.0180	0.0230	0.0229

Identification and evaluation of the COP model

The selection process as shown in Fig. 1 is also applied to search the most suitable COP model for the target variable-speed AC. The log-likelihoods of tested COP models in each iteration step are listed in Table 6. Like the selection process for cooling capacity model, the selection process for COP model also stops after two iterations. The first iteration stops at the test of M_5, which has a p-value less than 0.05. The M_4 is selected as the most suitable sub-model of COP^* in the first iteration, which has the largest p-value of 0.4369 and the minimum number of parameters of 6. In the second iteration, M_4 acts as the larger model and is compared with its restricted sub-models, i.e., M_8 and M_{12}. The iteration stops

at the test of M_8 vs. M_4 due to the p-value below 0.05. After the whole selection process for COP model M_4 is therefore chosen as the sufficient model as shown in Eq. (18).

$$COP^* = \frac{COP}{COP_{rated}} = \left(c_1 + c_2 T_{in,wb} + c_3 T_{out,db}\right) \times \left(1 + d_1 N_{comp} + d_2 N_{comp}^2 + d_3 N_{comp}^3\right) + \varepsilon_{COP} \quad (18)$$

The parameter estimates and performance indicators for candidate COP^* model is listed in Table 7. As can be seen from the table, the parameter estimates are different in various candidate COP^* models. Compared with M_5 and M_8, M_1- M_4 of COP^* have almost the same accuracy (RMSE and CV) and fitness (R^2) to the data. The RMSE, CV and R^2 for M_4 of COP^* are 0.0188, 0.0180 and 0.9954, respectively. However, M_4 of COP^* has the simplest model structure and the smallest number of parameters, i.e., 6.

Table 6. Likelihood ratio test results in the selection of COP^* model.

Iteration	Properties	Larger unrestricted model under H_1	Restricted sub-models under H_0			
0	Model number	M_1				
	No. of parameters	9				
	Log-likelihood	543.19				
1	Model number	M_1	M_2	M_3	M_4	M_5
	No. of parameters	9	8	7	6	8
	Degrees of freedom	/	1	2	3	1
	Log-likelihood	543.19	542.49	541.88	541.83	473.86
	p-value	/	0.2398	0.2708	0.4369	$<10^{-16}$
2	Model number	M_4	M_8			
	No. of parameters	6	5			
	Degrees of freedom	/	1			
	Log-likelihood	541.83	472.12			
	p-value	/	$<10^{-16}$			

Table 7. Parameter estimates and performance indicators for the candidate COP^* models.

		Model					
		M_1	M_2	M_3	M_4	M_5	M_8
Parameter estimates	a_1	3.5605	3.6824	3.5520	3.4922	3.0617	3.0030
	a_2	0.0089	0.0030	0.0030	0.0090	0.0076	0.0077
	a_3	-0.0351	-0.0391	-0.0303	-0.0303	-0.0301	-0.0260
	a_4	0.0001	0.0001	0.0001	/	0.0001	/
	a_5	0.0001	0.0001	/	/	0.0001	/
	a_6	-0.0002	/	/	/	-0.0002	/
	b_1	-0.0225	-0.0225	-0.0225	-0.0225	-0.0153	-0.0153
	b_2	0.0002	0.0002	0.0002	0.0002	0.0001	0.0001
	b_3	-9.64×10^{-7}	-9.64×10^{-7}	-9.64×10^{-7}	-9.64×10^{-7}	/	/
Performance indicators	*RMSE*	0.0464	0.0463	0.0463	0.0463	0.0575	0.0572
	R^2	0.9867	0.9867	0.9867	0.9867	0.9796	0.9795
	CV	0.0480	0.0480	0.0479	0.0479	0.0595	0.0592

As shown in Eqs. (17) – (18), the most suitable Q^* model and COP^* model of the target variable-speed AC have the same model structure, i.e., 3 influential variables and 6 parameters. The item of air temperatures ($T_{in,wb}$ and $T_{out,db}$) with first-order structure is competent and no quadratic or cross-coupling items are needed, while the most suitable item of compressor speed (N_{comp}) is a third order polynomial, which cannot be reduced for accuracy purpose. Note that it is not necessary that the cooling capacity and COP models have the same model structure, which depends on the measured data for identification. With the identified cooling capacity model and COP model, the power consumption of the variable-speed AC under specific operation condition can be obtained by dividing the cooling capacity by COP.

Conclusions

The balance between model accuracy and model simplicity is a critical issue in model identification. This paper presents a model selection approach to identify the simplified energy performance model of variable-speed ACs for building energy performance assessment as well as model-based FDD and optimal control. Likelihood ratio test, a statistical hypothesis testing method, is applied to compare the full model with a series of candidate sub-models. Maximum likelihood estimation is used to estimate the parameters of each candidate model. It has been shown that the approach is able to effectively select the cooling capacity and COP models for variable-speed ACs with reasonable complexity and satisfactory accuracy. The identified models have three variables and six parameters in total. The item of air temperatures is first order, while the item of compressor speed is third order. The RMSE and R^2 of the most suitable Q^* model are 0.0188 and 0.9954, respectively. The RMSE and R^2 of the most suitable COP^* model are 0.0463 and 0.9867, respectively.

Due to the simple structure, the identified suitable energy performance models of variable-speed ACs can be integrated with building thermal models to predict building thermal dynamics and energy consumption at both individual and large-scale levels. It can also serve as a power benchmark for fault detection and diagnosis of the operations of variable-speed ACs. Moreover, in the context of smart grid, it can be embedded in the smart home energy management systems for model-based optimal control in response to the dynamic penalty signals from electrical grids such as price signal and CO_2 intensity signal, which can help the residential customers to achieve financial benefits.

Different from conventional research work on model selection, which compared and identified the best model from a series of candidate models with different structures, the model selection approach developed in this study focuses on the selection of suitable polynomial regression models of variable-speed ACs. Most existing energy performance models of residential spilt-type ACs used in optimal control, FDD and demand response are in the form of polynomial functions considering the trade-off between computational efficiency and accuracy. In the future, we will collect the experimental data of various variable-speed ACs under a range of weather conditions and operating frequencies to further test the model selection approach .

Nomenclature

A	area, m^2
AC	air conditioner
C	orifice coefficient
c	specific heat, J/K
COP	coefficient of performance
CV	coefficient of variance
dim	dimension
D	Diameter, m
DR	demand response
EEV	electronic expansion valve
FDD	fault detection and diagnosis
H	hypothesis
h	enthalpy
L	likelihood function
LRT	likelihood ratio test
M	model
m	parameter number in larger model
$\dot{m}$	mass flow rate, kg/s
MLE	maximum likelihood estimation
N	compressor rotational speed
p	probability density function
P	pressure, Pa
Q	cooling capacity of air conditioner, W
r	parameter number in sub-model
R^2	coefficient of determination
$RMSE$	root mean square error
RTU	rooftop unit
SC	sub-cooling degree, ℃
SH	superheat degree, ℃

sup	supremum function
T	temperature, ℃
U	heat transfer coefficient, W/(m^2·K)
V	effective displacement volume, m^3
W	power consumption, W
X	variable vector

Greek symbols

α	parameter vector
ε	measurement error
ε	heat transfer effectiveness
η	compressor efficiency
λ	likelihood ratio
σ	variance
χ^2	chi-squared distribution

Subscripts

cond	condenser
comp	compressor
db	dry-bulb
evap	evaporator
ex	heat exchanger
i	inlet
in	indoor air
is	isentropic process
o	outlet
out	outdoor air
ov	overall
p	constant-pressure process
rated	rated condition
ref	refrigerant
ty	typical
v	expansion valve
v	constant-volume process
wb	wet-bulb

Funding

The research work presented in this paper is financially supported by a research grant (G-YBTB) in the Hong Kong Polytechnic University (PolyU) and the Strategic Focus Area (SFA) Scheme (1-BBW7)

of Research Institute for Sustainable Urban Development (RISUD) in PolyU. The support is gratefully acknowledged.

References

EMSD. (2018). Hong Kong Energy End-use Data 2018. *Electrical and Mechanical Services Department*.

Siddiqui O. (2009). Assessment of achievable potential from energy efficiency and demand response programs in the US (2010–2030). *Electric Power and Research Institute, January*.

FERC. (2009). A national assessment of demand response potential. *Federal Energy Regulatory Commission*.

FERC. (2018). Assessment of demand response and advanced metering. *Federal Energy Regulatory Commission*.

Thomas Auswin George, Jahangiri Pedram, Wu Di, Cai Chengrui, Zhao Huan, Aliprantis Dionysios C, & Tesfatsion Leigh. (2012). Intelligent residential air-conditioning system with smart-grid functionality. *Smart Grid, IEEE Transactions on, 3*(4), 2240-2251.

Wang Weimin, Katipamula Srinivas, Ngo Hung, & Underhill Ronald. (2019). Energy performance evaluation of variable-speed packaged rooftop units using field measurements and building energy simulation. *Energy and Buildings, 183*, 118-128.

Hu Maomao, & Xiao Fu. (2018). Price-responsive model-based optimal demand response control of inverter air conditioners using genetic algorithm. *Applied Energy, 219*, 151-164.

Li Yunhua, Liu Mingsheng, & Lau Josephine. (2015). Development of a variable speed compressor power model for single-stage packaged DX rooftop units. *Applied Thermal Engineering, 78*, 110-117.

Guo Yabin, Li Guannan, Chen Huanxin, Hu Yunpeng, Shen Limei, Li Haorong, Hu Min, & Li Jiong. (2017). Development of a virtual variable-speed compressor power sensor for variable refrigerant flow air conditioning system. *International Journal of Refrigeration, 74*, 73-85.

Hu Maomao, Xiao Fu, Jørgensen John Bagterp, & Wang Shengwei. (2019). Frequency control of air conditioners in response to real-time dynamic electricity prices in smart grids. *Applied Energy, 242*, 92-106.

Aynur Tolga N. (2010). Variable refrigerant flow systems: A review. *Energy and Buildings, 42*(7), 1106-1112.

Rasmussen B. P. (2005). *Dynamic modeling and advanced control of air conditioning and refrigeration systems.* (PhD), UIUC.

Yoon Ji Hoon, Bladick Ross, & Novoselac Atila. (2014). Demand response for residential buildings based on dynamic price of electricity. *Energy and Buildings, 80*, 531-541.

Li Shuhui, Zhang Dong, Roget Adam B, & O'Neill Zheng. (2014). Integrating home energy simulation and dynamic electricity price for demand response study. *Smart Grid, IEEE Transactions on, 5*(2), 779-788.

Faruqui Ahmad, & Sergici Sanem. (2010). Household response to dynamic pricing of electricity: a survey of 15 experiments. *Journal of Regulatory Economics, 38*(2), 193-225.

Wang D., Parkinson S., Miao W., Jia H., Crawford C., & Djilali N. (2013). Hierarchical market integration of responsive loads as spinning reserve. *Applied Energy, 104*, 229-238.

Taniguchi Ayako, Inoue Takuya, Otsuki Masaya, Yamaguchi Yohei, Shimoda Yoshiyuki, Takami Akinobu, & Hanaoka Kanako. (2016). Estimation of the contribution of the residential sector to summer peak demand reduction in Japan using an energy end-use simulation model. *Energy and Buildings, 112*, 80-92.

Lu Ning. (2012). An evaluation of the HVAC load potential for providing load balancing service. *Smart Grid, IEEE Transactions on, 3*(3), 1263-1270.

Zhang Wei, Lian Jianming, Chang Chin-Yao, & Kalsi Karanjit. (2013). Aggregated modeling and control of air conditioning loads for demand response. *Power Systems, IEEE Transactions on, 28*(4), 4655-4664.

Chen Zhi, Wu Lei, & Fu Yong. (2012). Real-time price-based demand response management for residential appliances via stochastic optimization and robust optimization. *Smart Grid, IEEE Transactions on, 3*(4), 1822-1831.

Alibabaei Nima, Fung Alan S., & Raahemifar Kaamran. (2016). Development of Matlab-TRNSYS co-simulator for applying predictive strategy planning models on residential house HVAC system. *Energy and Buildings, 128*, 81-98.

Shao Shuangquan, Shi Wenxing, Li Xianting, & Chen Huajun. (2004). Performance representation of variable-speed compressor for inverter air conditioners based on experimental data. *International Journal of Refrigeration, 27*(8), 805-815.

Cai Jie, & Braun James E. (2018). Assessments of variable-speed equipment for packaged rooftop units (RTUs) in the United States. *Energy and Buildings, 164*, 203-218.

Brandemuehl Michael J. (1993). *HVAC 2 toolkit : a toolkit for secondary HVAC system energy calculations*. Atlanta, Ga.: American Society of Heating, Refrigerating and Air-Conditioning Engineers.

Cheung Howard, & Braun James E. (2010). Performance Characteristics and Mapping for a Variable-Speed Ductless Heat Pump.

Bacher Peder, & Madsen Henrik. (2011). Identifying suitable models for the heat dynamics of buildings. *Energy and Buildings, 43*(7), 1511-1522.

Yu F. W., Ho W. T., Chan K. T., & Sit R. K. Y. (2018). Theoretical and experimental analyses of mist precooling for an air-cooled chiller. *Applied Thermal Engineering, 130*, 112-119.

Casella George, & Berger Roger L. (2002). *Statistical inference* (2nd ed.). Pacific Grove, CA: Duxbury.

Pawitan Yudi. (2001). *In all likelihood : statistical modelling and inference using likelihood*: Oxford University Press.

Myung In Jae. (2003). Tutorial on maximum likelihood estimation. *Journal of Mathematical Psychology, 47*(1), 90-100.

Cherem-Pereira G., & Mendes N. (2012). Empirical modeling of room air conditioners for building energy analysis. *Energy and Buildings, 47*, 19-26.

Meissner José W., Abadie Marc O., Moura Luís M., Mendonça Kátia C., & Mendes Nathan. (2014). Performance curves of room air conditioners for building energy simulation tools. *Applied Energy, 129*, 243-252.

Gayeski Nicholas Thomas. (2010). *Predictive pre-cooling control for low lift radiant cooling using building thermal mass.* Massachusetts Institute of Technology.

Choi J. M., & Kim Y. C. (2003). Capacity modulation of an inverter-driven multi-air conditioner using electronic expansion valves. *Energy, 28*(2), 141-155.

He Xiang-Dong, Liu Sheng, Asada H. Harry, & Itoh Hiroyuki. (1998). Multivariable control of vapor compression systems. *HVAC&R Research, 4*(3), 205-230.

Rasmussen Bryan P., & Alleyne Andrew G. (2004). Control-Oriented Modeling of Transcritical Vapor Compression Systems. *Journal of dynamic systems, measurement, and control, 126*(1), 54-64.

Zakula Tea, Gayeski Nicholas Thomas, Armstrong Peter Ross, & Norford Leslie Keith. (2011). Variable-speed heat pump model for a wide range of cooling conditions and loads. *HVAC&R Research, 17*(5), 670-691.

Zhou Rongliang, Zhang Tiejun, Catano Juan, Wen John T., Michna Gregory J., Peles Yoav, & Jensen Michael K. (2010). The steady-state modeling and optimization of a refrigeration system for high heat flux removal. *Applied Thermal Engineering, 30*(16), 2347-2356.

MathWorks. (2012). MATLAB and Statistics Toolbox Release: Natick, MA: The MathWorks.

Bell Ian H., Wronski Jorrit, Quoilin Sylvain, & Lemort Vincent. (2014). Pure and Pseudo-pure Fluid Thermophysical Property Evaluation and the Open-Source Thermophysical Property Library CoolProp. *Industrial & Engineering Chemistry Research, 53*(6), 2498-2508.

Appendix A. Physical modeling of variable-speed ACs

A.1. Steady-state models of the components in variable-speed ACs

A steady-state AC model is developed in this study to predict the coupled dynamic behaviors of the room and the AC under time-varying internal and external conditions. The steady-state performances of variable-speed AC in terms of cooling capacity and COP can be determined from compressor frequencies (N_{comp}) as well as indoor and outdoor air temperature ($T_{air,out}$ and $T_{air,in}$). For simplification of modeling, only the four major components, i.e. condenser, evaporator, variable- speed compressor, and electronic expansion valve (EEV), are modeled in this paper. Other minor components such as accumulator, refrigerant pipeline, sub-cooler and receiver are not considered here.

- *Variable-speed compressor*

Refrigerant mass flow rate and enthalpy at the compressor outlet are the key outputs of the compressor module. The refrigerant mass flow rate through the compressor and the refrigerant enthalpy at the compressor outlet are given by Eqs. (A.1) - (A.2), respectively.

$$\dot{m}_{comp} = N_{comp} V_{comp} \rho_{comp} \eta_v \tag{A.1}$$

$$h_{comp,o} = h_{comp,i} + \left(h_{comp,o,is} - h_{comp,i}\right)/\eta_{is} \tag{A.2}$$

where N_{comp}, V_{comp}, ρ_{comp} are the rotational speed of compressor motor in Hz, effective displacement volume, and refrigerant density at the inlet, respectively; $h_{comp,i}$, $h_{comp,o}$ are the enthalpies at the compressor inlet and outlet; $h_{comp,o,is}$ is the enthalpy at the compressor outlet under an isentropic compression; η_v and η_{is} are compressor volumetric efficiency and isentropic efficiency which can be approximately calculated by Eqs. (A.3) - (A.4), respectively.

$$\eta_v = 1 + c_{comp} - c_{comp}\left(P_{comp,o}/P_{comp,i}\right)^{\frac{c_v}{c_p}} \tag{A.3}$$

$$\eta_{is} = c_0 + c_1 N_{comp} + c_2 N_{comp}^2 + c_3 P_r + c_4 P_r^2 \tag{A.4}$$

where $P_{comp,o}$ and $P_{comp,i}$ are the refrigerant pressures at the compressor outlet and inlet, respectively; P_r is the ratio of compressor outlet pressure to the inlet pressure; c_{comp} is the compressor clearance ratio; c_v and c_p are the constant volume and constant pressure specific heats at the compressor inlet, respectively; c_0- c_4 are coefficients which can be empirically identified from the actual compressor.

- *Electronic expansion valve*

Expansion devices are used in the refrigeration systems to regulate the refrigerant mass flow rate into the evaporator and maintain the refrigerant superheat at the evaporator outlet. In recent years, due to its superior performance in control, EEV has been implemented in the variable-speed ACs or heat pumps to control the cooling capacity and superheat instead of the conventional expansion devices such as capillary tubes and thermostatic expansion valves (Choi & Kim, 2003). Refrigerant mass flow rate through an EEV can be modeled using Eq. (A.5). Since refrigerant expansion process in EEV can be considered as being adiabatic, the enthalpy at the EEV outlet therefore can be given by Eq. (A.6).

$$\dot{m}_v = C_v A_v \sqrt{\rho_v \left(P_{cond} - P_{evap}\right)} \tag{A.5}$$

$$h_{v,o} = h_{v,i} \tag{A.6}$$

where C_v, A_v, ρ_v are the orifice coefficient, valve opening area, refrigerant density, respectively; P_{cond} and P_{evap} are refrigerant pressures at the condenser and evaporator, respectively; $h_{v,o}$ and $h_{v,i}$ are the refrigerant enthalpies at the EEV inlet and outlet, respectively.

- *Heat exchangers*

The moving boundary approach is used here to model the thermal dynamics of the refrigerant in the heat exchangers, which is widely adopted for both transient modeling (B. P. Rasmussen, 2005; He et al., 1998; Bryan P. Rasmussen & Alleyne, 2004) and steady-state modeling (Zakula et al., 2011; Zhou et al., 2010) of heat exchangers. The method can capture the characteristics of multiple fluid phase heat exchangers while preserving the simplicity of lumped parameter models. The condenser is normally divided into three zones based on the refrigerant state, i.e. de-superheated, two-phase, and subcooled zones, and the evaporator is divided into two zones, i.e. two-phase and superheated zones. With these assumptions, the one-dimensional steady state model of each zone can be represented by the conservation equations of mass and energy, which only contain the derivatives to the length of the zones. After integration along the length, the steady state model of a heat exchanger zone can then be transformed into the two algebraic equations as follows:

$$\dot{m}_{ex,o} = \dot{m}_{ex,i} \tag{A.7}$$

$$h_{ex,o} = h_{ex,i} + Q_{ref,air}/\dot{m}_{ex,i} \tag{A.8}$$

where $\dot{m}_{ex,i}$ and $\dot{m}_{ex,o}$ are the mass flow rates at the inlet and outlet of the zone, respectively; $h_{ex,i}$ and $h_{ex,o}$ are the enthalpy at the inlet and outlet of the zone, respectively; $Q_{ref,air}$ is the heat exchanged

between the refrigerant and the air in that zone (negative value for the condenser). The heat transfer rates, $Q_{ref,air}$, in heat exchangers are calculated by effectiveness-number of transfer units (ε-NTU). The details of ε-NTU method and heat transfer correlations can be found in (Hu & Xiao, 2018).

How to determine the length of each zone is a critical issue for steady-state heat exchanger modeling using moving boundary approach. Details of the numerical solution for heat exchanger modeling can be found in Appendix A.2. Like the heat exchanger models, the solution for the modeling of the whole refrigeration system is implicit and can only be solved by a numerical method which shown in Appendix A.3.

A.2. Numerical solution for heat exchangers

A one-dimensional optimization technique is adopted here to determine the length of each zone in the heat exchangers and obtain the refrigerant enthalpy at the heat exchanger outlet. The heat transfer from the refrigerant to the air can be calculated by forwardly using the ε-NTU method. The length of each zone can be determined using the ε-NTU method inversely, as shown in Eqs. (A.9) - (A.10). The flow chart for numerical solution of heat exchangers is shown in Fig. A.1.

$$L = \frac{C_{min}}{U_{ov}\pi D_o(c_r-1)} ln \frac{Q_{max}-Q_{ref,air}}{Q_{max}-rQ_{ref,air}} \tag{A.9}$$

$$Q_{ref,air} = \dot{m}_{ex,i}\left(h_{ex,o} - h_{ex,i}\right) \tag{A.10}$$

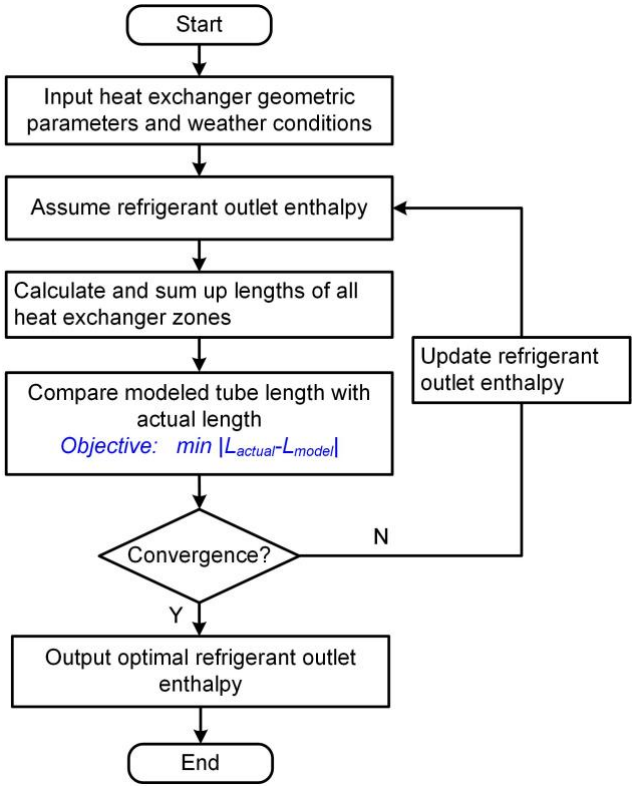

Fig. A.1. Flow chart for numerical solution of heat exchangers.

A.3. Numerical solution for the whole refrigeration system

Fig. A.2 shows the flowchart of the numerical solution of the whole refrigeration system. First, we input the geometric parameters of all components and operating conditions including the actuator signal, i.e. compressor rotational speed (N_{comp}) and environmental disturbances ($T_{air,out}$ and $T_{air,in}$). In the steady-state modeling of variable-speed AC, the condenser airflow rate and evaporator airflow rate are assumed to be constants under all operating conditions and are not manipulated in any situations. The EEV opening degree N_v, condenser pressure P_{cond}, evaporator pressure P_{evap} , sub-cooling degree at the condenser outlet SC, and superheat at the evaporator outlet SH under the specific operating conditions, i.e. $T_{air,out}$, $T_{air,in}$ and N_{comp}, are determined by a constrained nonlinear optimization, as shown in Fig. A.2. The reference values for sub-cooling (SC_{ref}) and superheat (SH_{ref}) are both 4.5°C which normally occurs in the real case. Given a set of N_v, P_{cond}, P_{evap}, SC and SH the nonlinear optimizer sequentially calls the modules of the compressor, condenser, EEV and evaporator and computes the value of the objective function as shown in Eq. (A.11).

$$\min_{N_v,P_{cond},P_{evap},SC,SH} \left(\frac{\dot{m}_{comp}-\dot{m}_v}{\dot{m}_{comp}}\right)^2 + \left(\frac{SC-SC_{ref}}{SC_{ref}}\right)^2 + \left(\frac{SH-SH_{ref}}{SH_{ref}}\right)^2 \tag{A.11}$$

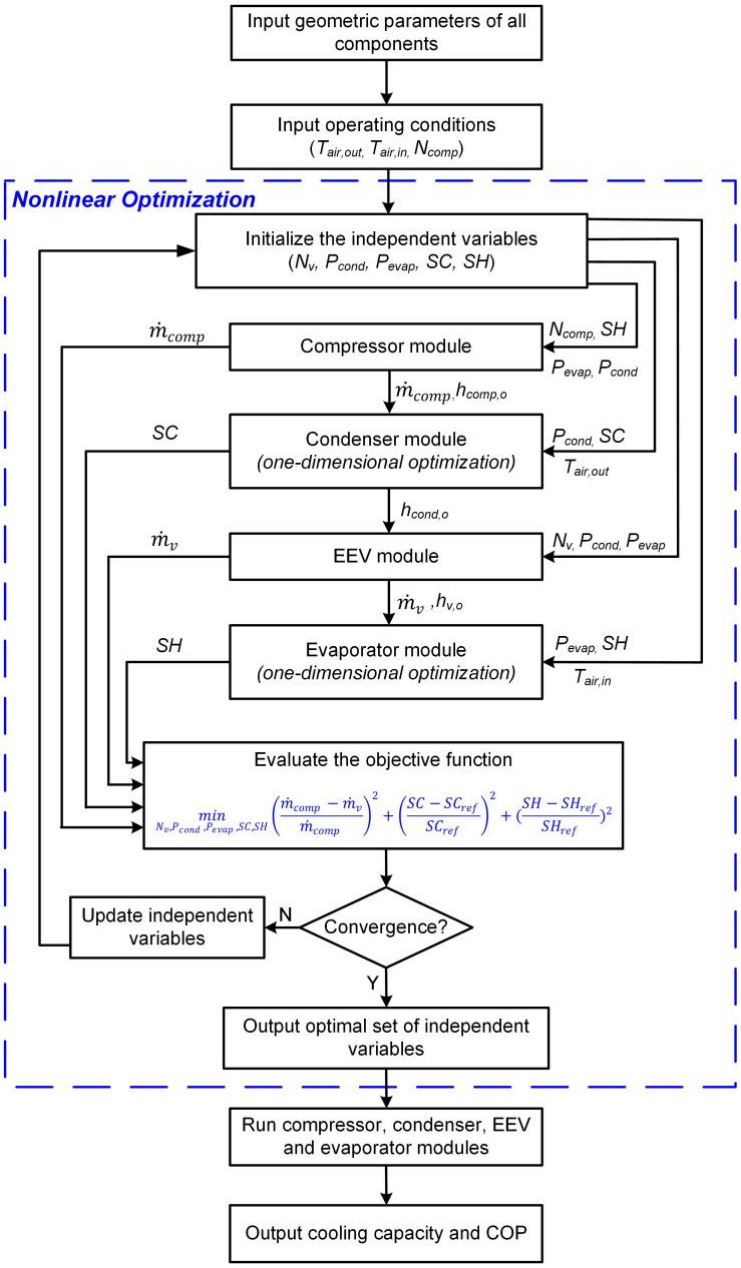

Fig. A.2. Flow chart for numerical solution of whole refrigeration system.

The outputs of the nonlinear optimization are then brought back to the refrigeration system from compressor to condenser, EEV and evaporator. To the end, the cooling capacity and COP under specific operating conditions can be calculated. In this study, all the component models of the refrigeration system and optimizations are carried out in MATLAB (MathWorks, 2012). The thermo-physical properties of refrigerant are calculated with the assistance of CoolProp tool (Bell et al., 2014).